RESEARCH

BMAL1 ameliorates type 2 diabetes-induced cognitive impairment via AREG upregulation and PI3K/Akt/GSK-3β pathway activation

Jialu Xu[1,2†], Chunyu Li[1,2†], Rongping Fan[1,2†], Jiaxin Yin[1,2], Lei Xie[1,2,3], Xuemin Peng[1,2], Jing Tao[1,2], Weijie Xu[1,2], Shujun Zhang[1,2], Xiaoli Shi[1,2], Kun Dong[1,2], Xuefeng Yu[1,2], Xi Chen[1,2*] and Yan Yang[1,2*]

Abstract

Cognitive impairment is a significant complication of type 2 diabetes mellitus (T2DM). However, the mechanisms underlying the development of cognitive dysfunction in individuals with T2DM remain elusive. Herein, we discussed the role of *Bmal1*, a core circadian rhythm-regulating gene, in the process of T2DM-associated cognitive dysfunction. We identified a marked decrease in BMAL1 levels in the hippocampus of db/db mice, followed by gain- and loss-of-function studies to explore the impact of BMAL1 on cognitive function. Our findings indicated that BMAL1 downregulation led to cognitive deficits, characterized by tau hyperphosphorylation and accumulated amyloid plaque. Conversely, BMAL1 overexpression mitigated these Alzheimer-like pathologies. Further investigation revealed that BMAL1 directly activated the transcription of *Areg*, thereby activating the PI3K/Akt/GSK-3β pathway and ameliorating cognitive dysfunction. Moreover, these effects of BMAL1 were attenuated by LY294002, a PI3K inhibitor. Collectively, these results underscore the significant role of BMAL1 in T2DM-associated cognitive impairment, proposing a novel intervention strategy for individuals exposed to risk factors of T2DM.

Keywords BMAL1, T2DM-associated cognitive impairment, AREG/PI3K/Akt/GSK-3β pathway

†Jialu Xu, Chunyu Li and Rongping Fan
contributed equally to this work and should be considered co-first authors.

*Correspondence:
Xi Chen
amazingamycx@163.com
Yan Yang
yangyan6910@163.com
[1] Department of Endocrinology, Tongji Hospital, Tongji Medical College, Huazhong University of Science and Technology, Wuhan, Hubei 430030, China
[2] Branch of National Clinical Research Center for Metabolic Diseases, Hubei, China
[3] Department of Endocrinology and Metabolism, GuiQian International General Hospital, Guiyang, China

Background

Type 2 diabetes mellitus (T2DM) is characterized by hyperglycemia and insulin resistance and is accompanied by several complications, including cognitive decline, cardiovascular disease, and so on. The global prevalence of diabetes among adults aged 20–79 years has been estimated at 10.5% [1]. Alzheimer's disease (AD) is a neurodegenerative disorder characterized by progressive cognitive decline. It is estimated that 6.2 million Americans aged 65 years or more are affected by AD, which brings a great burden to public health [2]. Epidemiological evidence suggests that individuals with T2DM are at a heightened risk of developing cognitive impairment, ranging from mild cognitive impairment to AD [3, 4]. People with T2DM have a 1.5 to 2.5 times increased risk of cognitive impairment compared to the general population [5]. Hyperglycemia induced by T2DM can

Xu *et al. Cell Communication and Signaling*　　　(2025) 23:7

Page 2 of 17

cause structural and functional alterations in neurons within the brain, leading to cognitive dysfunction [6]. Regrettably, clinical trials have demonstrated that managing blood glucose levels has limited positive impacts on cognition [7]. Although certain hypoglycemic medicines have shown promise in ameliorating cognitive dysfunction in individuals with T2DM, their treatments for cognition remain in the exploratory phase [8]. Therefore, novel potential mechanisms and new therapeutic targets for T2DM-associated cognitive impairment are urgently needed to be explored.

Recently, a close link between circadian disruption, T2DM, and cognitive impairment has been raised [9, 10]. Growing evidence highlights the role of circadian disturbance in cognitive decline [11, 12]. For instance, chronic sleep deprivation in mice has been shown to impair learning and memory [12]. Time-restricted feeding rescues brain pathology and improves memory in Alzheimer's disease mice [13]. The mechanisms by which circadian disruption accelerates cognitive decline have found an interesting direction in the Brain and Muscle Arnt-like 1(BMAL1) deficient animal model [14]. BMAL1, a central role in the circadian system, acts as a transcription factor that heterodimerizes with circadian locomotor output cycles kaput (CLOCK), another circadian gene, to activate circadian gene expression and maintain circadian rhythm [15, 16]. BMAL1-knockout animals showed circadian arrhythmicity [17] and cognitive impairments [18]. Our previous study has demonstrated the deleterious effects of circadian disruption in T2DM [19], wherein diabetic mice with disrupted circadian rhythm exhibited accelerated cognitive dysfunction and AD progression, along with disrupted BMAL1 expression rhythm. However, the impact of BMAL1 on cognitive dysfunction in individuals with T2DM has not been addressed and the underlying mechanisms remain unclear.

In this study, we investigated the role of BMAL1 in cognitive function, particularly within the context of T2DM. We observed that downregulation of BMAL1 had detrimental effects on cognition and accelerated the progression of Alzheimer-like pathology in db/db mice. Conversely, BMAL1 overexpression was associated with improved cognitive function. Moreover, our results showed BMAL1 activated *Amphiregulin (Areg)* transcription, inducing activation of the phosphoinositide 3-kinase (PI3K)/protein kinase B (Akt)/glycogen synthase kinase 3 beta (GSK-3β) signaling pathway. These findings highlight the crucial role of BMAL1 in cognitive function and suggest that activating the BMAL1-AREG signaling axis may serve as a potential strategy to enhance cognitive function in T2DM.

Materials and methods
Animals
Forty specific pathogen-free animals (SPF) male db/db mice (BKS-Lepr^{em2Cd479}/Gpt, strain number: T002407) aged 8 weeks and forty wt mice aged 8 weeks were obtained from the GemPharmatech Co., Ltd. (Jiangsu, China). Mice, housed 4–5 per cage, were allowed ad libitum access to normal food and water during the two-week acclimation period in a 12:12 light/dark cycle. For the first set animals, mice were randomized to subgroups as follows (1) wt-Con knockdown (KD), (2) wt-BMAL1 KD, (3) db/db-Con KD, (4) db/db-BMAL1 KD, (5) wt-Con overexpression (OE), (6) wt-BMAL1 OE, (7) db/db-Con OE, (8) db/db-BMAL1 OE, (n = 8 per group). After acclimation of two weeks, mice were injected with adeno-associated virus (AAV)-PHP. eB carrying either BMAL1 knockdown or overexpressing constructs through the tail vein (Fig. 1A). For the second set animals, mice were randomized to four groups: (1) db/db-Con OE + saline, (2) db/db-BMAL1 OE + saline, (3) db/db-Con OE + LY294002, (4) db/db-BMAL1 OE + LY294002 (n = 8 per group). Similarly, after acclimation of two weeks, mice were injected with AAV-PHP. eB carrying BMAL1 overexpressing constructs or control AAV through tail vein and intraperitoneally received PI3K inhibitor LY294002 (5 mg/kg) (purchased from MedChemExpress) or the same volume vehicle once a day. After 8 weeks, behavior tests were performed to explore the effect of BMAL1 on cognitive function in the eight groups before they were sacrificed. All animal experiments were approved by the Animal Care and Use Committee of Tongji Hospital (Approval number: TJH-202110034).

(See figure on next page.)

Fig. 1 BMAL1 downregulation exacerbated cognitive impairment. **A** The experimental timeline. **B, C** Western blots and quantitation analysis of the protein levels of BMAL1 (n = 3 per group). **D** Body weight (n = 8 per group). **E** Fasting blood glucose (n = 8 per group). **F, G** Blood glucose levels during GTT and ITT (n = 7 per group). **H, I** The total distance traveled and average velocity was assessed in the open field test (n = 8 per group). **J, K** The duration and frequency of exploring the novel object were assessed in the novel object recognition test (n = 8 per group). **L, M** Acquisition errors and probe errors of the Barnes maze test were assessed for spatial learning ability (n = 8 per group). Data were plotted as means ± SEM. *P < 0.05, **P < 0.01, ***P < 0.001. The data were analyzed by two-way ANOVA followed by post hoc Tukey's HSD test

Xu *et al. Cell Communication and Signaling*   (2025) 23:7
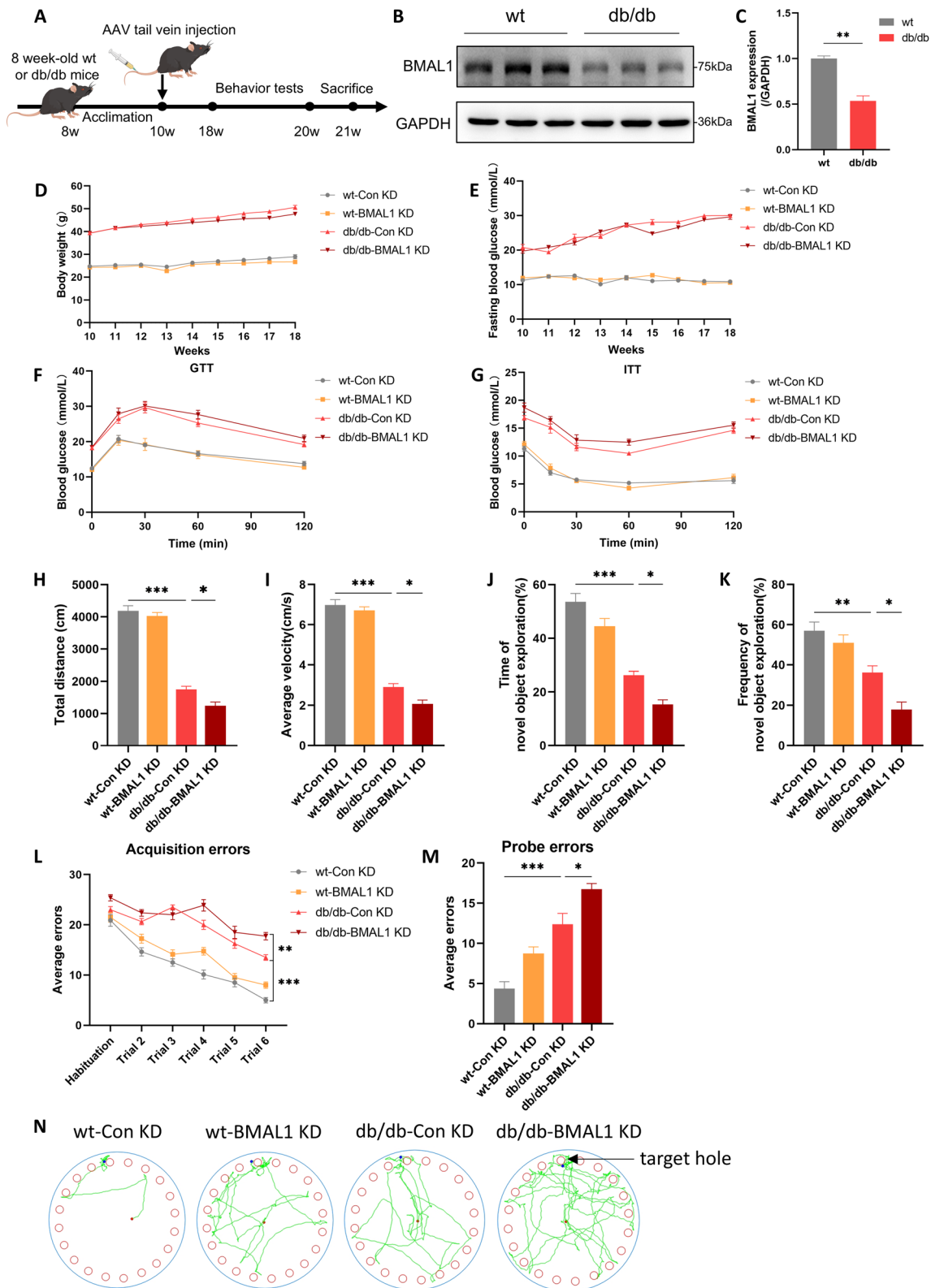
Page 3 of 17

Fig. 1 (See legend on previous page.)

AAV and tail vein injection

AAV-PHP.eB-CMV promoter-EGFP-MIR155(MCS)-SV40PolyA-*Bmal1* and AAV-PHP.eB-CMV-betaGlobin-MCS-3Flag-SV40PolyA-*Bmal1* vectors were purchased from GeneChem Company. Mice were anesthetized with isoflurane and injected intravenously with AAV-PHP.eB (3.0×10^{11} vg/mL per mouse) in a volume of 100 µl diluted by 0.9% NaCl after the tail was swabbed with alcohol.

Glucose tolerance tests (GTT) and insulin tolerance tests (ITT)

Mice were fasted for sixteen hours and then given an intraperitoneal injection of glucose (1.0 g/kg body weight, Hubei Kelun Pharmaceutical Co., Ltd.) in GTT. Six hours fasted mice were injected with human insulin (1 unit/kg Jiangsu Wanbang Biochemical Pharmaceutical Co., Ltd.) in ITT. Blood glucose concentrations were measured at 0, 15, 30, 60, and 120 min after injection by a blood glucose meter (ACCU-CHEK, Roche, Germany).

Behavioral tests

The behavioral tests were adapted according to our previous study [19]. On day 1, the open field test was conducted to assess general activities. On day 2, the novel object recognition test was used to detect hippocampal-related contextual learning ability. On day3-7, the Barnes maze test was performed to explore spatial learning and memory ability.

Open field test

For each trial, a mouse was placed in a $45 \times 45 \times 45$ cm square open field box and allowed 10 min to freely explore. The mouse's movements were recorded using an overhead video camera. The recorded data were then analyzed with the VisuTrack Animal Behavior Analysis System (XinRuan Co. Ltd., Shanghai) to determine the total distance traveled and the velocity of each mouse. To maintain cleanliness, the testing area was wiped with 75% ethanol between trials.

Novel object recognition test

In the initial trial, each mouse had 5 min to independently explore two identical objects within the open field. Afterward, the mouse was returned to its home cage and allowed a 30-min interval. In the subsequent trial, the mice were presented with two objects: one familiar and the other novel. They were given 5 min to explore both objects. The resulting data were expressed as the percentage of time spent investigating the novel object. This frequency was calculated as: [(frequency of investigating the novel object) / (total frequency of investigating both objects) * 100].

Barnes maze test

A Barnes maze consists of a circular platform (100 cm in diameter) elevated 90 cm above the floor. The platform, dark gray in color, featured 20 holes (5 cm in diameter), one of which led to an escape box. Spatial cues were

Table 1 Antibody information

Antibodies	Source and catalog number	Country	Dilution
Primary antibodies			
Tau5	Abcam, Cat # ab80579	Cambridge, UK	1:1000
p-Ser396	Abcam, Cat # ab109390	Cambridge, UK	1:10000
p-Thr231	Abcam, Cat # ab151559	Cambridge, UK	1:10000
p-Ser199	Abcam, Cat # ab81268	Cambridge, UK	1:10000
GAPDH	AntGene, Cat # ANT325	Wuhan, China	1:10000
APP	ABclonal, Cat #A17911	Wuhan, China	1:1000
BACE1	ABclonal, Cat #A11533	Wuhan, China	1:1000
BMAL1	Cell Signaling Technology, Cat #14020S	Boston, USA	1:1000
PI3K	Proteintech, Cat # 60225–1–Ig	Wuhan, China	1:10000
Phospho-PI3K (Tyr458) /p55 (Tyr199)	Cell Signaling Technology, Cat # 4228	Boston, USA	1:1000
Anti-AKT1 + AKT2 + AKT3	Abcam, Cat # ab179463	Cambridge, UK	1:10000
Anti-AKT1 (Phospho-S473)	Abcam, Cat # ab81283	Cambridge, UK	1:10000
GSK-3β	ABclonal, Cat # A11731	Wuhan, China	1:1000
Phospho-GSK-3β (Ser9)	ABclonal, Cat # AP1088	Wuhan, China	1:1000
Amphiregulin (Areg)	Proteintech, Cat # 16036–1–AP	Wuhan, China	1:1000
Secondary antibodies			
HRP-conjugated Affinipure Goat Anti-Mouse IgG(H + L)	Proteintech, Cat # SA00001-1	Wuhan, China	1:5000
HRP-conjugated Affinipure Goat Anti-Rabbit IgG(H + L)	Proteintech, Cat # SA00001-2	Wuhan, China	1:5000

Xu *et al. Cell Communication and Signaling*   (2025) 23:7

Page 5 of 17

placed around the platform to ensure visibility for the mice during the test. The Barnes maze protocol comprised two phases: "Spatial Acquisition" and "Probe Trials". On the first day, the mice were given 5 min to familiarize themselves with the maze. After a 30-min interval, the first acquisition session commenced, lasting 5 min. If the mice failed to locate the escape box within the allotted time, they were gently guided to it and allowed to remain there for 2 min. Over the second and third days, the mice underwent two 5-min training trials each day, with a 30-min inter-trial interval. The fourth day served as a rest day. On the fifth day, a probe test was conducted: the escape box was removed, and the mice were given 5 min to explore the maze. The number of errors made by each mouse before locating the escape hole was recorded using a video camera and analyzed with VisuTrack Animal Behavior Analysis System (XinRuan Co. Ltd., Shanghai) to assess spatial memory retention.

Western blots

The total protein was extracted from hippocampus samples with RIPA extract buffer containing protease and phosphatase inhibitors (Boster, China). The collected supernatants were centrifuged at $12,000 \times g$ for 15 min at 4 ℃ and then the protein concentration was measured via a bicinchoninic acid (BCA) kit (Boster, China). Proteins in the extracts (20 ug for each sample) were separated in 10% SDS-PAGE and transferred to a PVDF membrane (Millipore, China) at 300 mA. After blocking with the blocking buffer for one hour at room temperature, the membranes were incubated overnight with primary antibodies at 4 ℃. After being washed with tris-buffered saline with tween 20 (TBST) buffer three times, the membranes were incubated with secondary antibodies for one and a half hours. Information of antibodies is presented in Table 1. Finally, protein bands were visualized with an enhanced chemiluminescence detection kit (Biosharp, China) and detected with a GelView 6000 Pro (Antpedia, China). Band density was analyzed using ImageJ software.

Enzyme-linked immunoassay (ELISA)

ELISAs of Aβ1-40 and Aβ1-42 were performed as per the manufacturer's instructions (Elabscience, Wuhan, China). Briefly, frozen hippocampal tissues were homogenized in RIPA lysis buffer containing protease and phosphatase inhibitors (Boster, Wuhan, China), followed by centrifugation at 20,000 g for 30 min at 4 ℃. The supernatants were collected as soluble fractions. The levels of Aβ1-40 and Aβ1-42 were measured using ELISA kits (E-EL-M3009 and E-EL-M3010, Elabscience) according to the manufacturer's instructions.

Immunohistochemical (IHC) analysis

Mouse brains were collected on ice after sacrifice, and the right brain was removed and fixed in 4% paraformaldehyde. Paraffin-embedded brain tissues were sectioned. After the procedure of dewaxing, hydration, and antigen retrieval, sections were incubated with 10% goat serum (Boster#AR1009) for 20 min at room temperature. Then, the sections were immunostained with anti-beta Amyloid 1–42 antibody (1:200, Abcam# ab201061) overnight at 4 ℃ followed by incubation of a secondary antibody (1:2000, Abcam#ab205718) for 45 min at 37 ℃, and developed using diaminobenzidine (Maxim #DAB4033). Sections were counter-stained with hematoxylin, and IHC images were taken under a microscope (Olympus #CX31).

RNA extraction and Quantitative real time polymerase chain reaction (qRT-PCR)

We extracted total RNA from the hippocampus using Trizol reagent (Biosharp, Beijing, China). RNA concentration and quality were evaluated using a spectrophotometer (Denovix, USA). Subsequently, we synthesized cDNA using the Hifair II Reverse Transcription System and following the manufacturer's protocol (Yeasen Biotech Co. Ltd, Shanghai, China). QRT-PCR was conducted using the SYBR Green qPCR Master Mix (Tolo Biotech Co. Ltd, Shanghai, China) and QuantStudioTM 1 system (Thermo Fisher Scientific biosystem). Gene expression was normalized using glyceraldehyde 3-phosphate dehydrogenase (Gapdh), and the relative gene expression was calculated using the Comparative CT method $(2 - \Delta CT)$.

RNA sequencing (RNA-seq) analysis

Total RNA of the hippocampus of db/db mice with or without BMAL1 knockdown was extracted by Trizol (Biosharp, Beijing, China). A minimum of 2 µg RNA was sent to BGI Tech (Wuhan, China) for quality control, library preparation, and next-generation sequencing.

(See figure on next page.)

Fig. 2 BMAL1 overexpression improved cognitive deficits. **A** Body weight ($n = 8$ per group). **B** Fasting blood glucose ($n = 8$ per group). **C**, **D** Blood glucose levels during GTT and ITT ($n = 7$ per group). **E**, **F** The total distance traveled and average velocity was assessed in the open field test ($n = 8$ per group). **G**, **H** The duration and frequency of exploring the novel object were assessed in the novel object recognition test ($n = 8$ per group). **I**, **J** Acquisition errors and probe errors of the Barnes maze test were assessed for spatial learning ability ($n = 8$ per group). Data were plotted as means ± SEM. *$P < 0.05$, **$P < 0.01$, ***$P < 0.001$. The data were analyzed by two-way ANOVA followed by post hoc Tukey's HSD test

Xu *et al. Cell Communication and Signaling*   (2025) 23:7
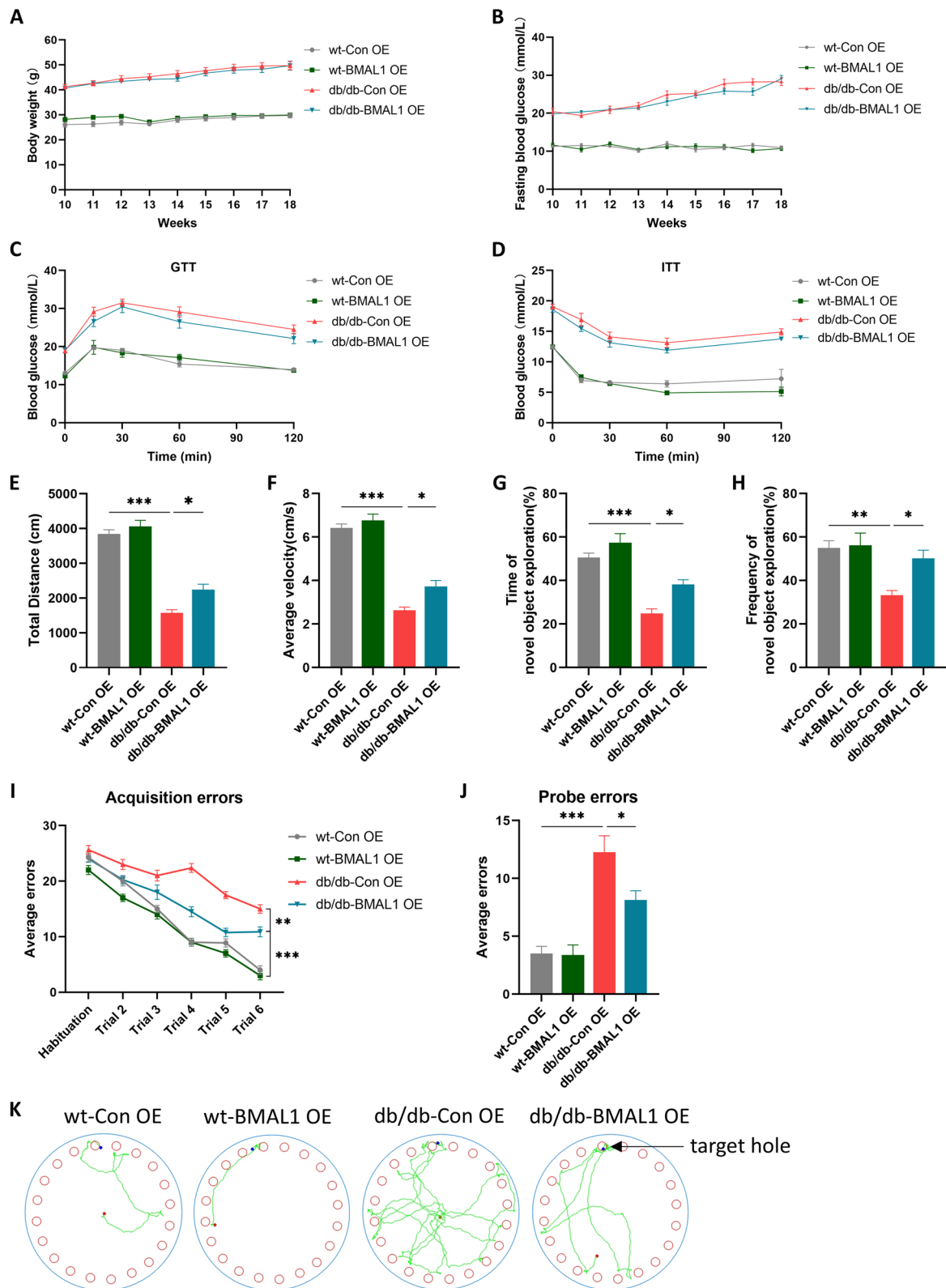
Page 6 of 17

Fig. 2 (See legend on previous page.)

In brief, the RNA was segmented into 250–300 bp fragments and reverse transcribed to cDNA. Next, the cDNA was subjected to PCR for amplification. After the PCR product was denatured to a single chain, the cyclization reaction system was prepared to obtain the single-chain ring product. Transcriptome sequencing was performed with the Novaseq platform (Illumina, USA), which generated 150 bp paired-end reads. The read numbers were counted by featureCounts v1.5.0-p3, followed by the calculation of FPKM of each gene. Differential gene testing between the two groups was performed using DESeq2 (v1.4.5) with p-value ≤ 0.05. And we use kyoto encyclopedia of genes and genomes (KEGG) enrichment analysis (https://www.kegg.jp/), with p value ≤ 0.05 as the threshold. Those meeting this condition are defined as significantly enriched in candidate genes.

Chromatin Immunoprecipitation (ChIP)

ChIP was conducted with Sonication ChIP Kit (Abclonal, RK20258). HT22 cells were crosslinked with 1% formaldehyde, followed by split and sonicated to shear the chromatin. Then it was incubated with ChIP grade anti-BMAL1 antibody (Cell Signaling TECHNOLOGY) or IgG for 4 h at 4 °C. After washing, the antibody-protein-DNA complexes were separated from the beads. Subsequently, the complexes were decrosslinked for 4 h at 65 °C, and DNA was purified.

Plasmid transfection and luciferase reporter assay

The pGL3-basic vector containing the *Areg* promotor (2000 bp) and HA-*Bmal1* (purchased from GENE-CHEM) plasmid were constructed. Based on the pGL3-*Areg* promoter (2000 bp), we further constructed site-mutant plasmids in which the sequence CACGGG (-60 to -45 bp) or CAGGTG (-20 to -15 bp) was replaced by AGTTTT or AGTTGT. HT22 cells were seeded into a 12-well plate and cultured until 75% confluence was obtained. The firefly luciferase reporter plasmid (400 ng) and pRL-TK plasmids (20 ng) with or without HA-*Bmal1* plasmid were co-transfected into the cells by Lipo3000™ Transfection Reagent (1.5 µL/well). After 48 h incubation, the cells were lysed with the lysis buffer, and the Firefly and Renilla luciferase were measured via the dual luciferase reporter assay system (Promega) according to

standard protocols. Calculate the ratio of luminescence from the Firefly luciferase to the Renilla luciferase to assess the relative luciferase signal.

Statistical analysis

All values were presented as means ± SEM. Data were analyzed by two-way ANOVA with genotype and virus genotype as between-subject factors. For multiple comparisons, Tukey's post hoc method or Dunn's test was applied according to the result of the homogeneity of variance test. GraphPad Prism (version 8.0) was used to plot figures. The quantitative analysis of amyloid plaque in hippocampal sections was evaluated using ImageJ software (Version 1.8.0.112, NIH, Bethesda, Maryland, USA). P values are represented as follows: $*P < 0.05$, $**P < 0.01$, $***P < 0.001$.

Results

BMAL1 downregulation exacerbated T2DM-associated cognitive impairment

Consistent with other studies, we observed a downregulation of BMAL1 in the hippocampus in db/db mice (Fig. 1B, C). To further elucidate the role of BMAL1, both gain- and loss-of-function studies were conducted. Ten-week-old wt mice or db/db mice were administered injections of either AAV-*Bmal1* knockdown or AAV-vector. As expected, db/db mice exhibited a higher body weight compared to wt mice, but BMAL1 knockdown did not affect the body weight in either wt mice or db/db mice (Fig. 1D). Consistently, db/db mice showed elevated fasting blood glucose compared to wt mice, yet there were no significant differences between BMAL1-KD and CON-KD groups (Fig. 1E). Subsequently, we conducted GTT and ITT tests to determine the impact of BMAL1 knockdown on glucose tolerance and insulin resistance. Obviously, BMAL1 knockdown did not influence glucose tolerance either in wt mice or db/db mice (Fig. 1F, G).

Following 8 weeks of AAV injection, open field test, novel object recognition test, and Barnes maze test were performed to explore the impact of BMAL1 knockdown on cognitive function. Compared to wt mice, db/db mice traveled shorter distances and exhibited lower average velocity. Furthermore, downregulation of BMAL1 further reduced both the total distance traveled and average

(See figure on next page.)

Fig. 3 BMAL1 knockdown aggravated Alzheimer-like pathology. **A**, **B** Western blots and quantitation analysis of the phosphorylation levels of tau at Ser396, Thr231, and Ser199 ($n = 4$ per group). **C**, **D** Western blots and quantitation analysis of the expression levels of APP and BACE1 ($n = 4$ per group). **E**, **F** Immunohistochemical for Aβ plaques in the hippocampus of mouse and quantitation analysis in four groups (Scale bars = 400 µm in low-magnification and scale bars = 100 µm in high-magnification image) ($n = 3$ per group). **G** ELISA of Aβ1-40 and Aβ1-42 in the hippocampus ($n = 4$ per group). Data were plotted as means ± SEM. $*P < 0.05$, $**P < 0.01$, $***P < 0.001$. The data were analyzed by two-way ANOVA followed by post hoc Tukey's HSD test
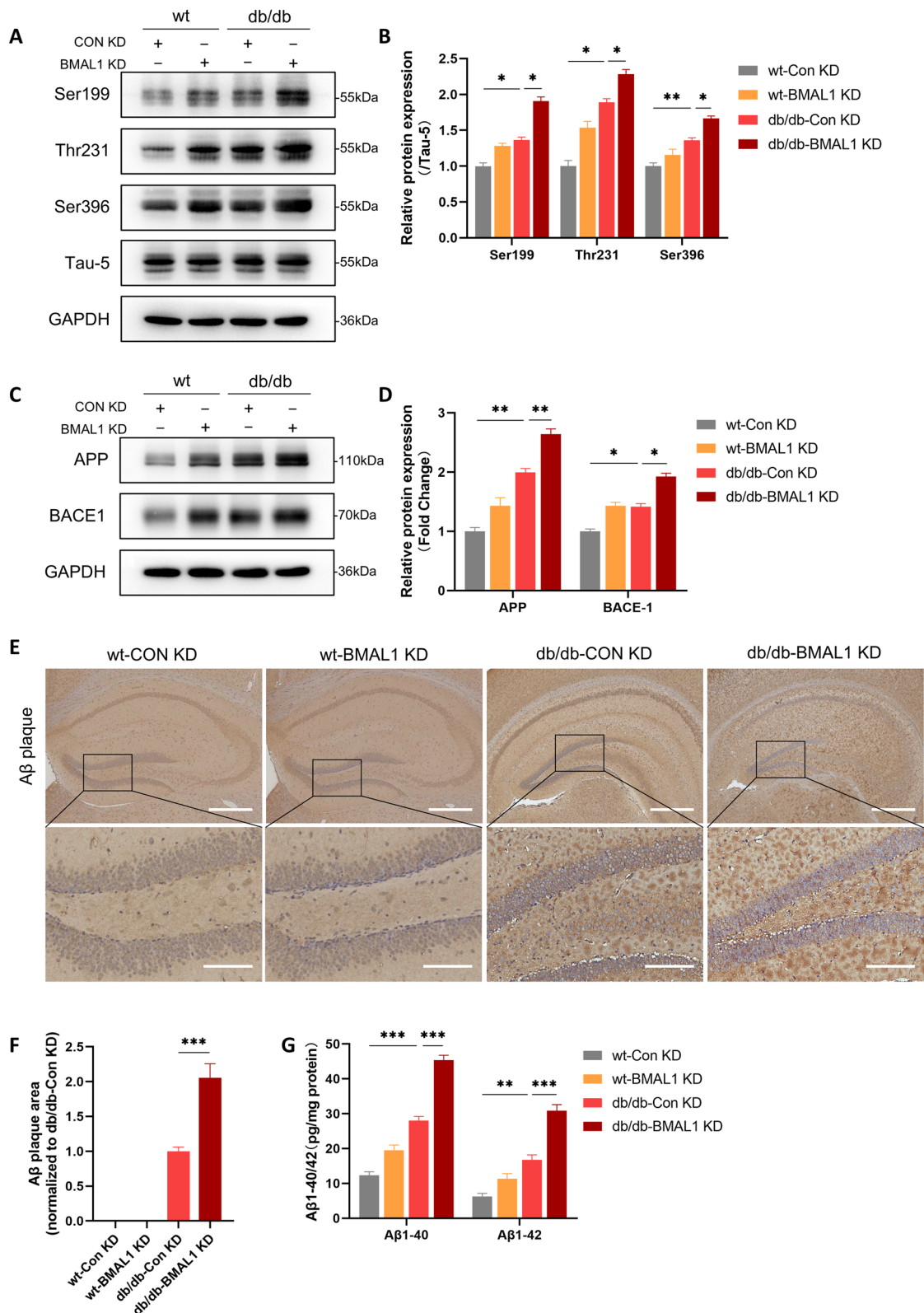
Fig. 3 (See legend on previous page.)

Xu *et al. Cell Communication and Signaling* (2025) 23:7

Page 9 of 17

velocity in db/db mice (Fig. 1H, I). In the novel object recognition test, db/db mice exhibited poorer performance than wt mice, indicating that diabetes impaired contextual learning. Furthermore, less exploration duration and the frequency of interactions with the novel object was observed in db/db-BMAL1 KD mice, highlighting the role of BMAL1 in contextual learning deficits (Fig. 1J, K). In the Barnes maze test for assessing spatial memory, db/db mice made more errors in acquisition trials than wt mice, and db/db-BMAL1 KD mice committed even more errors in acquisition trials (Fig. 1L). Similarly, in the probe trial conducted 24 h after rest, BMAL1 knockdown contributed to more errors (Fig. 1M, N). Taken together, BMAL1 knockdown exacerbates the cognitive function of db/db mice.

BMAL1 overexpression improved T2DM-associated cognitive deficits
Another batch of mice was treated with the AAV-*Bmal1* overexpression. Likewise, the body weight and fasting blood glucose of mice were recorded per week. It showed that BMAL1 overexpression did not increase or decrease body weight and there was no significant difference in fasting blood glucose between BMAL1-OE and CON-OE subgroups in both wt mice or db/db mice (Fig. 2A, B). Consistent with BMAL1 knockdown mice, the results of GTT and ITT showed that BMAL1 overexpression did not have an impact on glucose tolerance of insulin resistance (Fig. 2C, D).

Subsequently, behavior tests were conducted to determine the effect of BMAL1 overexpression on cognition. In the open field test, diabetes decreased the total distance traveled and average velocity, while BMAL1 overexpression slightly increased both parameters in db/db mice (Fig. 2E, F). In the novel object recognition test, db/db mice mice exhibited shorter exploration durations and less frequency of the novel object. However, BMAL1 overexpression mitigated these effects, indicating that BMAL1 overexpression enhances contextual learning ability (Fig. 2G, H). In the Barnes maze test, spatial memory deficits were observed in db/db mice, but BMAL1 upregulation improved it. Both in the acquisition trial and probe trial, BMAL1 overexpression led to fewer errors in db/db mice (Fig. 2I-K). Taken together, BMAL1 overexpression partially alleviates T2DM-associated cognitive function.

BMAL1 knockdown aggravated Alzheimer-like pathology
Hyperphosphorylation of tau and accumulation of amyloid β (Aβ) are two critical hallmarks of AD. Hyperphosphorylation of tau results from the abnormal phosphorylation of tau under pathological conditions, leading to the formation of intracellular neurofibrillary tangles. Accumulation of Aβ the latter derives from cleavage of the amyloid precursor protein (APP) by the β-site amyloid precursor protein cleaving enzyme-1 (BACE1), resulting in extracellular deposition of amyloid plaques [20]. Subsequently, we detected phosphorylation of tau protein and Aβ deposition in the hippocampus in mice to determine the impact of BMAL1 on Alzheimer-like pathology. We detected the phosphorylation levels of tau protein at the Ser396, Thr231, and Ser199 sites in four groups. It showed that diabetes increased the phosphorylation level of tau protein, and the tau hyperphosphorylation was greater when BMAL1 was knockdown (Fig. 3A, B).

We next examined whether BMAL1 knockdown influenced the hippocampal deposition of Aβ. The expression of APP and BACE1 was analyzed. APP expression was significantly elevated in db/db mice compared to wt mice, with the highest levels observed in the db/db-BMAL1 KD subgroup. Similar results were found for BACE1 expression, where db/db-BMAL1 KD mice exhibited higher levels of BACE1 compared to db/db mice (Fig. 3C, D). Additionally, amyloid plaques, another important pathological hallmark of AD, derived from BACE1-cleaved APP were detected in the brain. Aβ accumulation was notably higher in db/db mice, particularly in db/db-BMAL1 KD mice, while little to no amyloid plaque was observed in wt mice by immunohistochemistry. (Fig. 3E, F). ELISA analysis revealed increased levels of both Aβ1-40 and Aβ1-42 in the hippocampal homogenates of db/db mice, with a more pronounced increase in db/db-BMAL1 KD mice (Fig. 3G). These results indicated that downregulation of BMAL1 aggravates Aβ accumulation by upregulating APP and BACE1 levels in db/db mice, as well as tau hyperphosphorylation.

BMAL1 overexpression extenuated Alzheimer-like pathology
Subsequently, we plan to explore whether the upregulation of BMAL1 improves Alzheimer-like pathology in the hippocampus. As we expected, phosphorylation
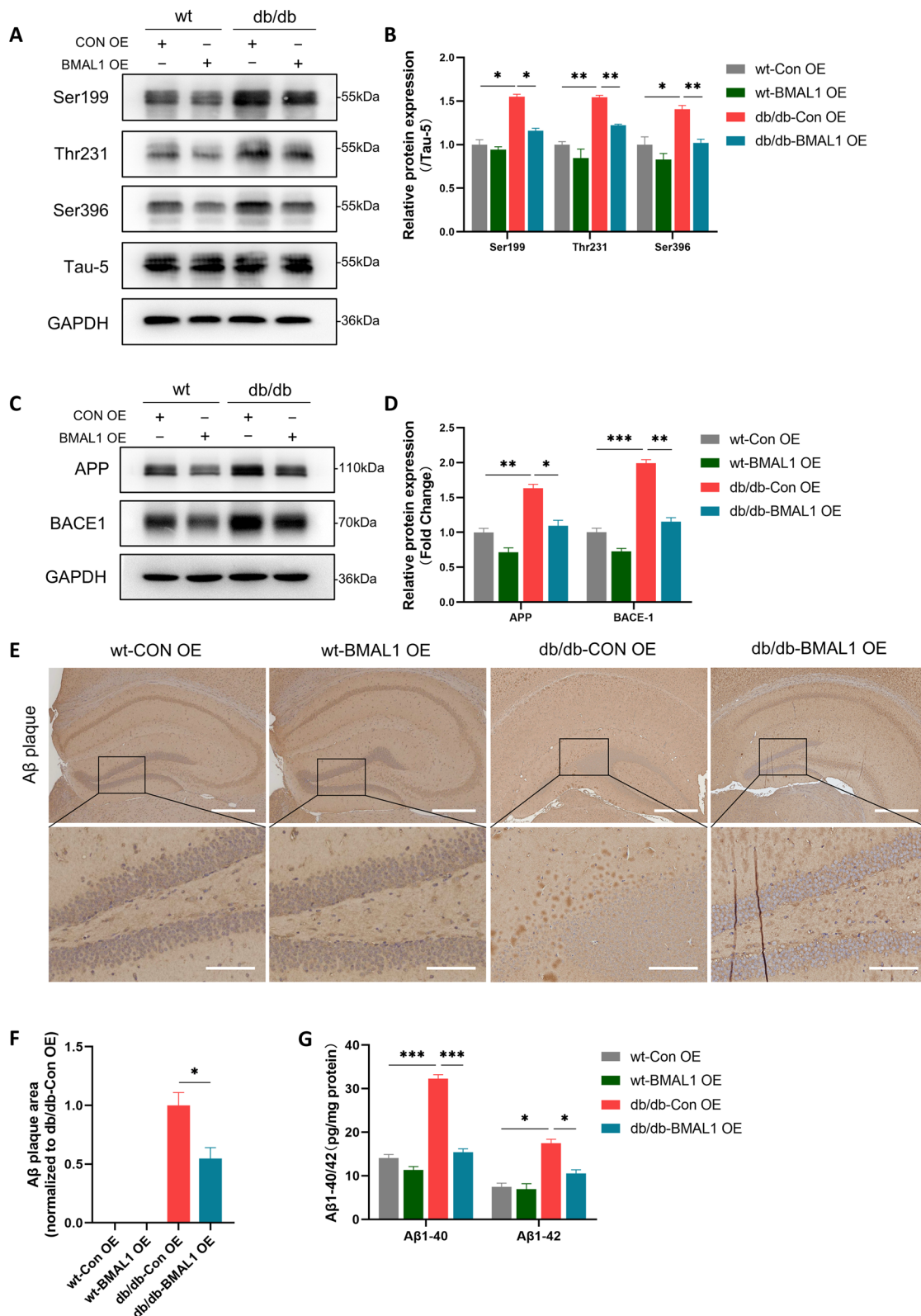
(See figure on next page.)
Fig. 4 BMAL1 overexpression extenuated Alzheimer-like pathology. **A**, **B** Western blots and quantitation analysis of the phosphorylation levels of tau at Ser396, Thr231, and Ser199 ($n = 4$ per group). **C**, **D** Western blots and quantitation analysis of the expression levels of APP and BACE1 ($n = 4$ per group). **E**, **F** Immunohistochemical for Aβ plaques in the hippocampus of mouse and quantitation analysis in four groups (Scale bars = 400 μm in low-magnification and scale bars = 100 μm in high-magnification image) ($n = 3$ per group). **G** ELISA of Aβ1-40 and Aβ1-42 in the hippocampus ($n = 4$ per group). Data were plotted as means ± SEM. *$P < 0.05$, **$P < 0.01$, ***$P < 0.001$. The data were analyzed by two-way ANOVA followed by post hoc Tukey's HSD test

Fig. 4 (See legend on previous page.)

levels of tau protein at the Ser396, Thr231, and Ser199 sites were elevated in db/db mice, while BMAL1 over-expression prevented this elevation (Fig. 4A, B). In line with this finding, upregulation of BMAL1 reduced the amyloid burden in the brain. Specifically, the levels of APP and BACE1 were lower in db/db-BMAL1 OE mice compared to db/db-Con OE mice (Fig. 4C, D). Immuno-histochemical analysis revealed a reduction in amyloid plaques in db/db-BMAL1-OE mice compared to db/db ConOE mice (Fig. 4E, F). Furthermore, the result of ELISA showed that BMAL1 overexpression reversed the elevated levels of Aβ1-40 and Aβ1-42 induced by T2DM (Fig. 4G).

BMAL1 activated AREG/PI3K/Akt/GSK-3β signaling pathway in db/db mice

To identify the underlying mechanisms by which BMAL1 influences cognition, we performed RNA-seq of CON-KD or BMAL1-KD hippocampus tissue of db/db mice to characterize the transcriptional profile of BMAL1 knockdown. KEGG analysis revealed that regulated genes enriched in pathways including PI3K-Akt signal-ing pathway, cytokine-cytokine receptor interaction, calcium signaling pathway, and so on (Fig. 5A). Among these pathways, PI3K/Akt signaling pathway has the most genes enriched. Prior research has identified the role of the PI3K/Akt/GSK-3β signaling pathway in tau hyperphosphorylation and amyloid plaque [21], and our study further confirmed the effect of BMAL1 on this pathway. In both wt and db/db mice, downregulation of BMAL1 markedly reduced the phosphorylation level of PI3K, Akt, and GSK-3β (Fig. 5B and Supplementary Fig. 1A). Interestingly, the administration of AAV-*Bmal1* overexpressing activated the pathway by increasing the phosphorylation level of PI3K, Akt, and GSK-3β (Fig. 5B and Supplementary Fig. 1B). These results indicated the significant role of PI3K/Akt/GSK-3β signaling pathway in BMAL1 knockdown-induced cognitive impairment.

Subsequently, we investigated the mechanisms by which BMAL1 regulates PI3K/Akt/GSK-3β signaling pathway. We focused on differentially expressed genes

(DEGs) involved in this process. A total of 1945 DEGs were identified in the BMAL1-knockdown hippocampus, including 588 downregulated genes and 1357 upregulated genes (Supplementary Fig. 1C). We identified 21 signifi-cantly downregulated and 23 significantly upregulated DEGs (Fig. 5C). Among these DEGs, we focused on *Areg*, an epidermal growth factor (EGF)-like gene. The AREG protein contains an EGF-like domain (amino acids 141–181) characterized by six spatially conserved cysteines that form disulfide bridges, defining the typical 3-looped structure of the EGF family [22], and a previous study has identified the effect of AREG on PI3K/Akt signaling activation [23]. QRT-PCR assays verified that BMAL1 knockdown downregulated *Areg*, whereas BMAL1 over-expression upregulated *Areg* both in wt and db/db mice significantly (Fig. 5D, E). Next, we examined the protein expression of AREG in the hippocampus and the results were consistent with qRT-PCR findings (Fig. 5F and Sup-plementary Fig. 1D-E).

BMAL1, a well-established transcription factor, exerts its function by activating downstream target genes [24]. To explore whether BMAL1 modulates the transcription of *Areg*, a dual-luciferase assay was per-formed and the results showed that BMAL1 activated the *Areg* promoter (Fig. 5G). To further investigate whether BMAL1 directly regulates *Areg*, we conducted ChIP and designed 10 primers of 200 bp (P1-P10) spanning the full-length *Areg* promoter to confirm the potential binding region (Fig. 5H). Subsequent PCR showed that the P10 region was crucial for BMAL1 binding to the *Areg* promoter (Fig. 5H). Additionally, using the JASPAR database, we identified two poten-tial BMAL1 binding sites on the Areg promoter, CAC GGG and CAGGTG (Fig. 5I). Then we constructed two promoter-mutant plasmids, MUT1 and MUT2, against these two binding sites, and co-transfected it with either vector or HA-*Bmal1* plasmid into HT22 cells. Dual-luciferase assay was then performed and the activity of MUT1 (AGTTTT) and MUT2 (AGT TGT) was partially decreased compared to WT, while the activity of double mutant (MUT1+MUT2) was

(See figure on next page.)

Fig. 5 BMAL1 activated AREG/PI3K/Akt/GSK-3β signaling pathway in db/db mice. **A** KEGG enrichment analysis of those DEGs in sequence data of control and BMAL1-KD hippocampus. **B** Western blots of the phosphorylation level of PI3K, Akt, and GSK-3β in the hippocampus of mice in the BMAL1-KD and BMAL1-OE groups (*n*=4 per group). **C** Heatmap showing the DEGs of control and BMAL1-KD hippocampus (**D**) Relative expression of *Bmal1* and *Areg* mRNA in the hippocampus of mice in the BMAL1-KD four groups (*n*=4 per group). **E** Relative expression level of *Bmal1* and *Areg* mRNA in the hippocampus of mice in the BMAL1-OE four groups (*n*=4 per group). **F** Western blots of protein level of BMAL1 and AREG in the hippocampus of mice in the BMAL1-KD and BMAL1-OE groups (*n*=3 per group). **G** Dual-luciferase reporter analysis of *Areg*-promoter plasmid co-transfecting with vector or HA-*Bmal1* (*n*=3 per group). **H** ChIP and PCR analysis of the interaction between BMAL1 and *Areg* promotor. **I** Binding sites of BMAL1-*Areg* promoter predicted by JASPAR. **J** Dual-luciferase reporter analysis of HA-*Bmal1* co-transfecting with WT *Areg*-promoter plasmid, or MUT1 (ATGGGG), or MUT2 (AGTTGT) (*n*=3 per group). Data were plotted as means±SEM. *$P < 0.05$, **$P < 0.01$, ***$P < 0.001$. The data were analyzed by two-way ANOVA followed by post hoc Tukey's HSD test
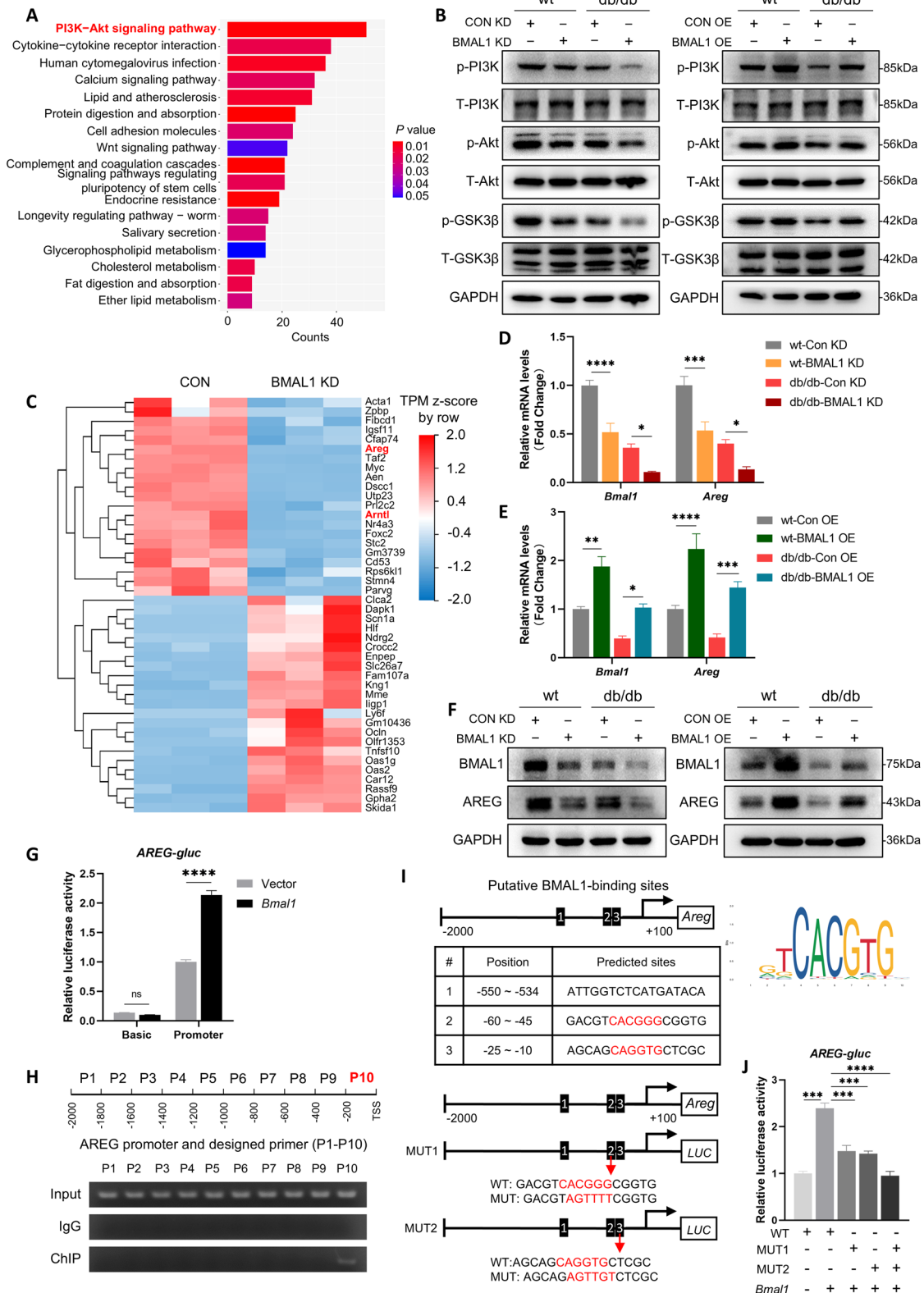
Fig. 5 (See legend on previous page.)

completely decreased (Fig. 5J). Collectively, these results demonstrate that BMAL1 binds to both identified sites and directly regulates the transcription of Areg.

BMAL1 overexpression improves cognition depends on PI3K/Akt/GSK-3β signaling pathway in db/db mice

To further confirm the reliance of BMAL1-mediated cognitive improvement on the PI3K/Akt/GSK-3β signaling pathway, we used LY294002, an inhibitor of PI3K on db/db mice (Fig. 6A). As expected in behavioral tests, treatment with LY294002 eliminated the BMAL1 overexpression-induced cognitive improvement. Consistent with prior results (Figs. 1 and 2), upregulation of BMAL1 increased the time and frequency of new objective exploration in novel objective recognition test, and decreased the errors in Barnes maze test (Fig. 6B-H). Conversely, inhibition of PI3K inhibited this effect, leading to a poorer cognitive function in LY294002-treatment BMAL1 overexpression db/db mice compared to non LY294002-treatment BMAL1 overexpression group (Fig. 6B-H). Moreover, we measured the activation of the PI3K/Akt/GSK-3β signaling pathway. Phosphorylation levels of PI3K, Akt, and GSK-3β were elevated by BMAL1 overexpression, however, this effect was diminished when LY294002 was used as expected (Fig. 6I and Supplementary Fig. 2A).

Subsequently, we investigated whether related pathology improved by BMAL1 upregulation depends on the PI3K/Akt/GSK-3β signaling pathway. BMAL1 overexpression protected tau protein from hyperphosphorylation at Ser199, Thr231, and Ser396 sites, but it failed when PI3K was inhibited (Fig. 6J and Supplementary Fig. 2B). Additionally, BMAL1 overexpression decreased APP and BACE1, which was reversed by inhibiting PI3K activation (Fig. 6K and Supplementary Fig. 2C). Furthermore, analysis of IHC revealed that LY294002 treatment increased Aβ plaque burden despite BMAL1 being upregulated (Fig. 6L and Supplementary Fig. 2D). Interestingly, ELISA of Aβ1-40 and Aβ1-42 showed similar results (Fig. 6M).

Discussion

In general, BMAL1 plays a vital role in variety of diseases, such as cardiovascular diseases, cancer, osteoarthrosis, and so on. It has been reported that BMAL1 downregulation leads to diabetic cardiomyopathy by promoting mitochondrial Ca^{2+} overload [25]. Shen et al. found that BMAL1 regulated the switch of vascular smooth muscle cells towards fibroblast-like cells to stabilize an atherosclerotic plaque [26]. Our previous study demonstrated that db/db mice exhibited impaired circadian rhythms, accompanied by the disappearance of circadian clock gene oscillations, such as *Bmal1* [27]. In this study, we first identified a reduction of BMAL1, a core circadian rhythm regulator, in db/db mice. Subsequently, gain- and loss-of-function experiments were further conducted to investigate the impact of BMAL1 on cognitive function and Alzheimer-like pathologies in db/db mice. We observed that BMAL1 knockdown exacerbated cognitive impairments, along with increased tau hyperphosphorylation, aggravated Aβ deposition by impairing AREG/PI3K/Akt/GSK-3β signaling pathway (Fig. 7). Conversely, BMAL1 overexpression exerted a therapeutic effect on cognitive function, markedly attenuating cognitive impairments and Alzheimer-like progression in db/db mice. To our knowledge, this study represents the first to elucidate the interaction between BMAL1 downregulation and diabetes in influencing cognitive impairments, offering new insights into the role of BMAL1 downregulation in the progression of cognitive impairment.

It has been reported that BMAL1 functions by activating downstream target genes. Li et al. found that BMAL1 binds to the E-box element in the promoter region of BCL2 interacting protein 3 (BNIP3) and BMAL1 knockout directly reduced BNIP3 protein level, causing mitochondria dysfunction and compromised cardiomyocyte function [28]. Chen et al. found that BMAL1 was the direct transcriptional activator of prolyl 4-hydroxylase subunit alpha 1 (P4ha1), orchestrating collagen prolyl hydroxylation and secretion in chondrocytes [24]. In this study, we revealed that BMAL1 directly combined with *Areg* promoter and activated the transcription of *Areg*.

(See figure on next page.)

Fig. 6 BMAL1 overexpression-induced cognitive improvement depends on PI3K/Akt/GSK-3β signaling pathway in db/db mice. **A** The experimental timeline. **B**, **C** The total distance traveled and average velocity was assessed in the open field test ($n=8$ per group). **D**, **E** The duration and frequency of exploring the novel object were assessed in the novel object recognition test ($n=8$ per group). **F**, **G** Acquisition errors and probe errors of the Barnes maze test were assessed for spatial learning ability ($n=8$ per group). **H** Representative track images of mice in the probe trial in the Barnes maze test. **I** Western blots of the phosphorylation levels of PI3K, Akt, and GSK-3β in the hippocampus ($n=3$ per group). **J** Western blots of the phosphorylation levels of tau at Ser396, Thr231, and Ser199 sites in the hippocampus ($n=3$ per group). **K** Western blots of the expression levels of APP and BACE1 in the hippocampus ($n=3$ per group). **L** Immunohistochemical for Aβ plaques in the hippocampus in four groups (Scale bars=400 μm in low-magnification and scale bars=100 μm in high-magnification image) ($n=3$ per group). **M** ELISA of Aβ1-40 and Aβ1-42 in the hippocampus ($n=4$ per group). Data were plotted as means±SEM. *$P<0.05$, **$P<0.01$, ***$P<0.001$. The data were analyzed by two-way ANOVA followed by post hoc Tukey's HSD test
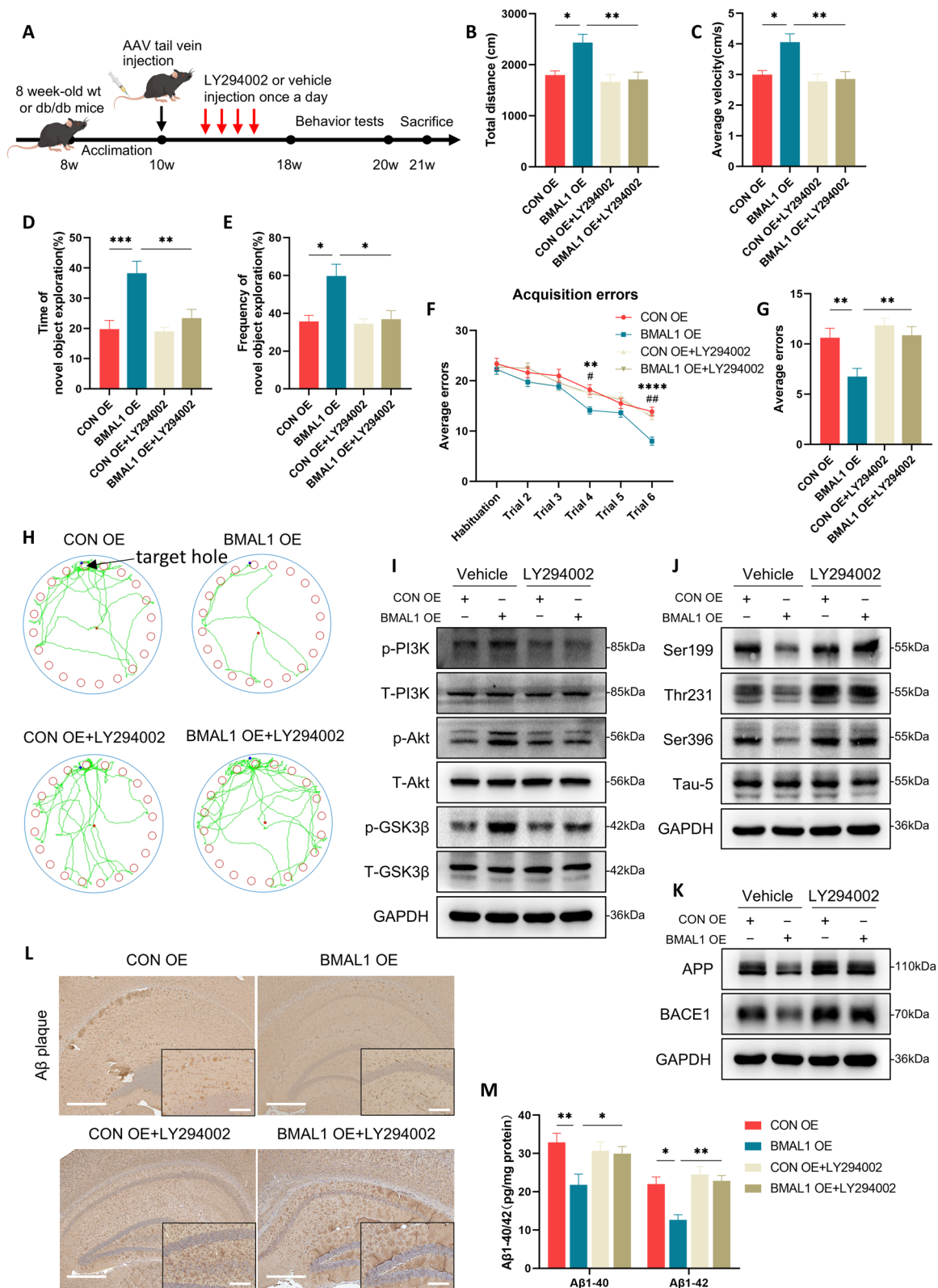
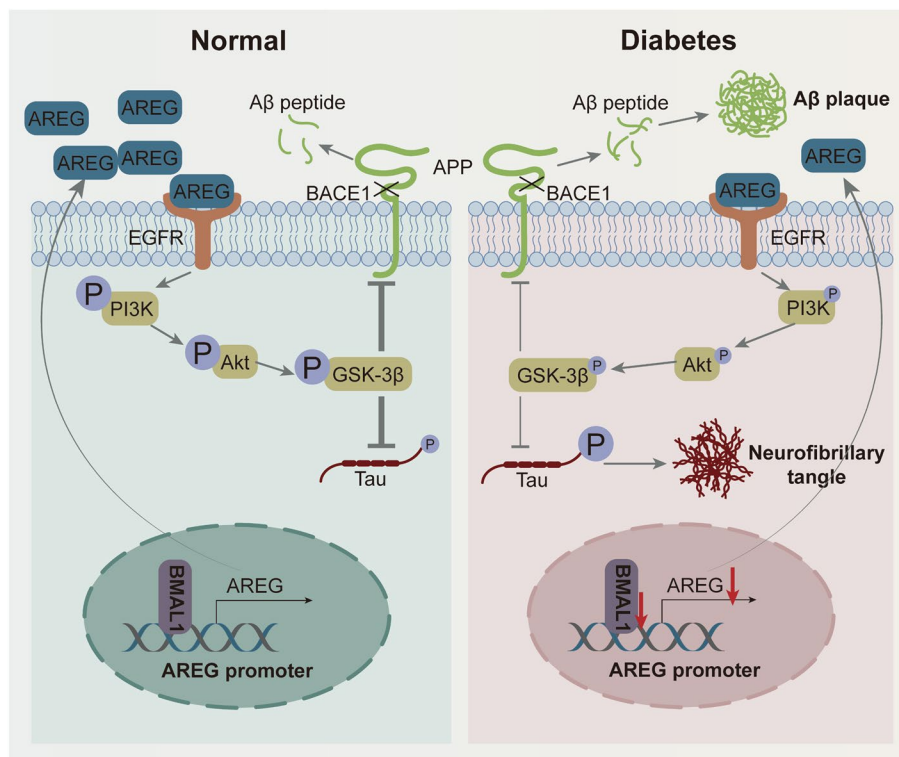**Fig. 6** (See legend on previous page.)

Fig. 7 Schematic illustration of the mechanism by which BMAL1 deficiency impairs cognitive function. BMAL1 downregulation induced by diabetes inhibits *Areg* transcription and the activation of the PI3K/Akt/GSK-3β signaling pathway in the hippocampus, inducing tau hyperphosphorylation, amyloid plaques, and cognitive dysfunction

The AREG protein contains an EGF-like domain (amino acids 141–181) capable of interacting with EGF receptors to initiate downstream signaling [22]. It plays an important role in cell proliferation, growth, differentiation, and repair [22].

PI3K/Akt/GSK-3β has been identified a significant role in AD [21]. GSK-3β, a critical protein kinase, modulates the function and stability of target proteins through phosphorylation [29]. As reported by previous studies, reduced GSK-3β phosphorylation promotes tau phosphorylation and Aβ accumulation [30, 31]. Here we demonstrated that BMAL1 activated the PI3K/Akt/GSK-3β signaling pathway. We observed significantly increased levels of tau phosphorylation in BMAL1-KD mice, while overexpression of BMAL1 decreased tau phosphorylation in db/db mice. Aβ deposition was escalated in db/db mice compared to wt mice, and further exacerbated in BMAL1-KD subgroups. Additionally, utilize of the PI3K inhibitor LY294002 diminished the therapeutic effect of BMAL1 overexpression, highlighting the significant role of the PI3K/Akt/GSK-3β pathway in cognitive improvement induced by BMAL1 overexpression in db/db mice.

This finding suggests that BMAL1 could be clinically utilized to treat cognitive impairment induced by T2DM. Literature reports suggest that certain foods, such as piperine [32], (-)-Epigallocatechin-3-gallate [33], and nobiletin [34], can enhance the expression of BMAL1, potentially guiding dietary strategies for patients with T2DM-induced cognitive deficits in clinical settings. Additionally, drugs such as melatonin and retinoic acid-related orphan receptor agonists have been shown to elevate BMAL1 levels in the brain, suggesting their potential for treating cognitive impairment induced by T2DM.

Overall, our study suggests for the first time that BMAL1 is a key molecule in T2DM-induced cognitive impairment, highlighting potential implications for clinical treatment. The present study offers several notable findings. Firstly, our study demonstrated that the interaction between BMAL1 knockdown and diabetes exacerbated cognitive impairments. This implies that exposure to circadian disruption and diabetes may constitute

Xu *et al. Cell Communication and Signaling*   (2025) 23:7

Page 16 of 17

critical risk factors contributing to the prevalence of cognitive impairments in industrialized societies. Secondly, we revealed BMAL1 transcriptionally regulated Areg and activated PI3K/Akt/GSK-3β pathway. Thirdly, BMAL1 overexpression ameliorated cognitive dysfunction in db/db mice, offering direct evidence that BMAL1 could be a therapeutic target for T2DM-induced cognitive decline. However, our study had limitations; we did not explore the underlying mechanisms of BMAL1 low expression in db/db mice and we may investigate it in future research.

Abbreviations

AD   Alzheimer's disease
AKT   Protein kinase B
APP   Amyloid precursor protein
AREG   Amphiregulin
Aβ   Amyloid β-protein
BACE1   β-Site amyloid precursor protein cleaving enzyme-1
BMAL1   Brain and muscle arnt-like 1
BNIP3   BCL2 interacting protein 3
CLOCK   Circadian locomotor output cycles kaput
DEGs   Differentially expressed genes
ELISA   Enzyme linked immunoassay
GAPDH   Glyceraldehyde 3-phosphate dehydrogenase
GSK-3β   Glycogen synthase kinase 3 beta
GTT   Glucose tolerance tests
IHC   Immunohistochemical
ITT   Insulin tolerance tests
KEGG   Kyoto encyclopedia of genes and genomes
KD   Knockdown
OE   Overexpression
PI3K   Phosphoinositide 3-kinase
QRT-PCR Quantitative real time polymerase chain reaction
RNA-seq RNA sequencing
SPF   Specific pathogen-free animals
TBST   Tris-buffered saline with tween 20
T2DM   Type 2 diabetes mellitus
WT   Wild-type

Supplementary Information

The online version contains supplementary material available at https://doi.org/10.1186/s12964-024-02019-5.

Supplementary Material 1: Supplementary Figure 1. (A) Quantification analysis of the phosphorylation levels of PI3K, Akt, and GSK-3β in the BMAL1-KD groups (*n*=4 per group). (B) Quantification analysis of the phosphorylation levels of PI3K, Akt, and GSK-3β in the BMAL1-OE groups (*n*=4 per group). (C) Volcano plot showed the DEGs between the control and BMAL1-KD hippocampus. (D) Quantification analysis of BMAL1 and AREG protein levels in the BMAL1-KD groups (*n*=3 per group). (E) Quantification analysis of BMAL1 and AREG protein levels in the BMAL1-OE groups (*n*=3 per group).

Supplementary Material 2: Supplementary Figure 2. (A) Quantification analysis of the phosphorylation levels of PI3K, Akt, and GSK-3β in the hippocampus (*n* = 3 per group). (B) Quantification analysis of the phosphorylation levels of tau at Ser396, Thr231, and Ser199 sites in the hippocampus (*n*=3 per group). (C) Quantification analysis of the expression levels of APP and BACE1 (*n*=3 per group). (D) Quantification analysis of immunohistochemical for Aβ plaques in the hippocampus (*n*=3 per group).

Data availability
No datasets were generated or analysed during the current study.

Declarations

Ethics approval and consent to participate
All animal experiments were approved by the Animal Care and Use Committee of Tongji Hospital (Approval number: TJH-202110034).

Consent for publication
Written informed consent was obtained from all participants in accordance with the Declaration of Helsinki.

Competing interests
The authors declare no competing interests.

References

1. Sun H, Saeedi P, Karuranga S, et al. IDF Diabetes Atlas: Global, regional and country-level diabetes prevalence estimates for 2021 and projections for 2045. Diabetes Res Clin Pract. 2022;183:109119. https://doi.org/10.1016/j.diabres.2021.109119. published Online First: 2021/12/10.
2. Alzheimer's Association. 2023 Alzheimer's disease facts and figures. Alzheimers Dement. 2023;19(4):1598-695. https://doi.org/10.1002/alz.13016. published Online First: 2023/03/16.
3. Alford S, Patel D, Perakakis N, et al. Obesity as a risk factor for Alzheimer's disease: weighing the evidence. Obes Rev. 2018;19(2):269–80. https://doi.org/10.1111/obr.12629.
4. Cukierman T, Gerstein HC, Williamson JD. Cognitive decline and dementia in diabetes–systematic overview of prospective observational studies. Diabetologia. 2005;48(12):2460–9.
5. van Gennip ACE, Stehouwer CDA, van Boxtel MPJ, et al. Association of type 2 diabetes, according to the number of risk factors within target range, with structural brain abnormalities, cognitive performance, and risk of dementia. Diabetes Care. 2021;44(11):2493–502. https://doi.org/10.2337/dc21-0149. published Online First: 2021/10/01.
6. Zhang S, Zhang Y, Wen Z, et al. Cognitive dysfunction in diabetes: abnormal glucose metabolic regulation in the brain. Front Endocrinol. 2023;14:1192602. https://doi.org/10.3389/fendo.2023.1192602. published Online First: 2023/07/03.
7. van Sloten TT, Sedaghat S, Carnethon MR, et al. Cerebral microvascular complications of type 2 diabetes: stroke, cognitive dysfunction, and depression. Lancet Diabetes Endocrinol. 2020;8(4):325–36. https://doi.org/10.1016/s2213-8587(19)30405-x. published Online First: 2020/03/07.
8. Cukierman-Yaffe T, Gerstein HC, Colhoun HM, et al. Effect of dulaglutide on cognitive impairment in type 2 diabetes: an exploratory analysis of the REWIND trial. Lancet Neurol. 2020;19(7):582–90. https://doi.org/10.1016/s1474-4422(20)30173-3. published Online First: 2020/06/21.
9. Peng X, Fan R, Xie L, et al. A growing link between circadian rhythms, type 2 diabetes mellitus and Alzheimer's disease. Int J Mol Sci. 2022;23(1):504. https://doi.org/10.3390/ijms23010504.
10. Karatsoreos IN, Bhagat S, Bloss EB, et al. Disruption of circadian clocks has ramifications for metabolism, brain, and behavior. Proc Natl Acad Sci U S A. 2011;108(4):1657–62. https://doi.org/10.1073/pnas.1018375108.

11. Musiek ES, Bhimasani M, Zangrilli MA, et al. Circadian rest-activity pattern changes in aging and preclinical Alzheimer disease. JAMA Neurol. 2018;75(5):582–90. https://doi.org/10.1001/jamaneurol.2017.4719.
12. Niu L, Zhang F, Xu X, et al. Chronic sleep deprivation altered the expression of circadian clock genes and aggravated Alzheimer's disease neuropathology. Brain Pathol (Zurich, Switzerland). 2022;32(3):e13028. https://doi.org/10.1111/bpa.13028. published Online First: 2021/10/21.
13. Whittaker DS, Akhmetova L, Carlin D, et al. Circadian modulation by time-restricted feeding rescues brain pathology and improves memory in mouse models of Alzheimer's disease. Cell Metab. 2023;35(10):1704-21.e6. https://doi.org/10.1016/j.cmet.2023.07.014. published Online First: 2023/08/23.
14. Kress GJ, Liao F, Dimitry J, et al. Regulation of amyloid-β dynamics and pathology by the circadian clock. J Exp Med. 2018;215(4):1059–68. https://doi.org/10.1084/jem.20172347.
15. Reinke H, Asher G. Crosstalk between metabolism and circadian clocks. Nat Rev Mol Cell Biol. 2019;20(4):227–41. https://doi.org/10.1038/s41580-018-0096-9.
16. Fan R, Peng X, Xie L, et al. Importance of Bmal1 in Alzheimer's disease and associated aging-related diseases: mechanisms and interventions. Aging Cell. 2022;21:e13704. https://doi.org/10.1111/acel.13704.
17. Yang G, Chen L, Grant GR, et al. Timing of expression of the core clock gene Bmal1 influences its effects on aging and survival. Sci Transl Med. 2016;8(324):324ra16. https://doi.org/10.1126/scitranslmed.aad3305.
18. Castro-Zavala A, Alegre-Zurano L, Cantacorps L, et al. Bmal1-knockout mice exhibit reduced cocaine-seeking behaviour and cognitive impairments. Biomed Pharmacother. 2022;153:113333. https://doi.org/10.1016/j.biopha.2022.113333.
19. Huang J, Peng X, Fan R, et al. Disruption of circadian clocks promotes progression of Alzheimer's disease in diabetic mice. Mol Neurobiol. 2021;58(9):4404–12. https://doi.org/10.1007/s12035-021-02425-7.
20. Busche MA, Hyman BT. Synergy between amyloid-β and tau in Alzheimer's disease. Nat Neurosci. 2020;23(10):1183–93. https://doi.org/10.1038/s41593-020-0687-6.
21. Baki L, Shioi J, Wen P, et al. PS1 activates PI3K thus inhibiting GSK-3 activity and tau overphosphorylation: effects of FAD mutations. EMBO J. 2004;23(13):2586–96. https://doi.org/10.1038/sj.emboj.7600251. published Online First: 2004/06/12.
22. Berasain C, Avila MA. Amphiregulin. Semin Cell Dev Biol. 2014;28:31–41. https://doi.org/10.1016/j.semcdb.2014.01.005. published Online First: 2014/01/28.
23. Xu Q, Long Q, Zhu D, et al. Targeting amphiregulin (AREG) derived from senescent stromal cells diminishes cancer resistance and averts programmed cell death 1 ligand (PD-L1)-mediated immunosuppression. Aging Cell. 2019;18(6):e13027. https://doi.org/10.1111/acel.13027. published Online First: 2019/09/08.
24. Chen G, Tang Q, Yu S, et al. Developmental growth plate cartilage formation suppressed by artificial light at night via inhibiting BMAL1-driven collagen hydroxylation. Cell Death Differ. 2023;30(6):1503–16. https://doi.org/10.1038/s41418-023-01152-x. published Online First: 2023/04/08.
25. Zhang N, Yu H, Liu T, et al. Bmal1 downregulation leads to diabetic cardiomyopathy by promoting Bcl2/IP3R-mediated mitochondrial Ca(2+) overload. Redox Biol. 2023;64:102788. https://doi.org/10.1016/j.redox.2023.102788. published Online First: 2023/06/25.
26. Shen Y, Xu LR, Yan D, et al. BMAL1 modulates smooth muscle cells phenotypic switch towards fibroblast-like cells and stabilizes atherosclerotic plaques by upregulating YAP1. Biochim Biophys Acta. 2022;1868(9):166450. https://doi.org/10.1016/j.bbadis.2022.166450. published Online First: 2022/05/23.
27. Huang J, Peng X, Fan R, et al. Disruption of circadian clocks promotes progression of Alzheimer's disease in diabetic mice. Mol Neurobiol. 2021;58(9):4404–12. https://doi.org/10.1007/s12035-021-02425-7. published Online First: 2021/05/22.
28. Li E, Li X, Huang J, et al. BMAL1 regulates mitochondrial fission and mitophagy through mitochondrial protein BNIP3 and is critical in the development of dilated cardiomyopathy. Protein Cell. 2020;11(9):661–79. https://doi.org/10.1007/s13238-020-00713-x. published Online First: 2020/04/12.
29. Hur EM, Zhou FQ. GSK3 signalling in neural development. Nat Rev Neurosci. 2010;11(8):539–51. https://doi.org/10.1038/nrn2870. published Online First: 2010/07/22.
30. Credle JJ, George JL, Wills J, et al. GSK-3β dysregulation contributes to parkinson's-like pathophysiology with associated region-specific phosphorylation and accumulation of tau and α-synuclein. Cell Death Differ. 2015;22(5):838–51. https://doi.org/10.1038/cdd.2014.179. published Online First: 2014/11/15.
31. Phiel CJ, Wilson CA, Lee VM, et al. GSK-3alpha regulates production of Alzheimer's disease amyloid-beta peptides. Nature. 2003;423(6938):435–9. https://doi.org/10.1038/nature01640. published Online First: 2003/05/23.
32. Zhang W, Ho CT, Lu M. Piperine improves lipid dysregulation by modulating circadian genes Bmal1 and clock in HepG2 cells. Int J Mol Sci. 2022;23(10):5611. https://doi.org/10.3390/ijms23105611. published Online First: 2022/05/29.
33 Mi Y, Qi G, Gao Y, et al. (-)-Epigallocatechin-3-gallate Ameliorates Insulin resistance and mitochondrial dysfunction in HepG2 cells: involvement of Bmal1. Mol Nutri Food Res. 2017;61(12):1700440. https://doi.org/10.1002/mnfr.201700440. published Online First: 2017/09/05.
34. Sulaimani N, Houghton MJ, Bonham MP, et al. Effects of (Poly)phenols on circadian clock gene-mediated metabolic homeostasis in cultured mammalian cells: a scoping review. Adv Nutr (Bethesda, Md). 2024;15:100232. https://doi.org/10.1016/j.advnut.2024.100232. published Online First: 2024/04/23.

Publisher's Note